Inorganica Chimica Acta 407 (2013) 131–138

Contents lists available at ScienceDirect

Inorganica Chimica Acta

journal homepage: www.elsevier.com/locate/ica

Synthesis and characterization of a series of rhodium, iridium, and ruthenium isocyanide complexes

Aaron P. Walsh, William W. Brennessel, William D. Jones *

Department of Chemistry, University of Rochester, Rochester, NY 14627, USA

ARTICLE INFO

Article history:
Received 17 May 2013
Received in revised form 16 July 2013
Accepted 18 July 2013
Available online 8 August 2013

Keywords:
Rhodium
Iridium
Ruthenium
Isocyanide

ABSTRACT

Several new electrophilic metal isocyanide complexes have been fully characterized and reported herein. Isocyanide induced cleavage of the dimer, $[LMCl_2]_2$ {LM = Cp*Ir, Cp*Rh, or (*p*-cymene)Ru}, with 2, 6-xylylisocyanide or 2,6-diethylphenylisocyanide produces complexes of the general formula $LM(CNAr)Cl_2$. Halide metathesis of the dichloro complexes with sodium iodide produces the corresponding complexes with the general formula $LM(CNAr)I_2$. For the analogous ruthenium complexes better results were achieved via isocyanide induced cleavage of $[(p\text{-cymene})RuI_2]_2$ and was synthesized differently from previous reports. Several neutral complexes in reaction with $AgPF_6$ in acetonitrile form cationic, solvent-coordinated complexes have been fully characterized. Most reactions with rhodium decomposed to either $[Cp^*RhCl(MeCN)]_2[(PF_6)_2]$ starting from the dichloro complexes, or $[Cp^*Rh(MeCN)_3,(PF_6)_2]$ and $Cp^*Rh(CNAr)I_2$ starting from the diiodo complexes. Several bases were probed to see if cyclization could be induced, but were not successful in any case. Many of these complexes have been characterized by single crystal X-ray crystallography.

1. Introduction

C–H bond functionalization via homogenous transition metal complexes has become an attractive approach in the synthesis of industrial & medicinally relevant compounds, especially synthesis and embellishment of heterocyclic compounds which are commonly found in natural products and drug molecules [1–4]. Functionalization of C–H bonds constitutes a more efficient synthetic tool avoiding pre-activated substrates, harsh reaction conditions, and disposal of toxic by-products and waste. For the past few decades, studies in C–H bond activation via transition metals has shown promising developments towards activating 'difficult' C–H bonds including (sp^3)C–H bonds [5–14]. Successful applications of C–H functionalization stem from a thorough mechanistic understanding of the C–H bond metalation based upon the nature of the active metal species.

For late transition metals C–H bond activation can occur via two pathways. The commonly employed oxidative addition in which an electron rich metal fragment inserts into a C–H bond, or electrophilic activation with an electron poor metal species assisted by a Lewis-basic ligand such as a carboxylate [15–18]. Specifically carboxylate-assisted electrophilic C–H activation has become a very powerful protocol due to the mild conditions and stability of organometallic intermediates making for an easily studied system [19]. Significant work done by Fagnou [16,20,21], Ackermann [22–25], and Ellman [26–31] describes the broadening scope, utility, and understanding of carboxylate-assisted C–H bond functionalizations. Our group has developed and exploited a few procedures via electrophilic activation using $[Cp^*MCl_2]_2$ [M = Ir (**1**); Rh (**2**)] to stoichiometrically synthesize polycyclic isoquinoline salts [32] and probe the mechanism and selectivity of these cyclometallations [33]. Furthermore, the reactivity of cyclometalated intermediates with small molecules and regioselectivity of the insertion has been studied [34].

Recently we have also shown competent H/D exchange with novel electrophilic rhodium and iridium complexes possessing a *fac*-chelating bis-pyrazolylacetate ligand with benzene and other substituted arenes [35]. Similarly studies with Tp′Ir (Tp′ = hydrotris(3,5-dimethylpyrazolyl)borate) [36–38] and one case with **1** [39] show benzylic C–H activation via iridium(III). With these precedents we wanted to explore the potential reactivity of **1** and **2** with aryl isocyanides such as 2,6-xylyl isocyanide, in which electrophilic activation of a benzylic (sp^3)C–H bond followed by cyclization could lead to indole products, as seen earlier with ruthenium(0) (Fig. 1) [40,41].

2. Results and discussion

2.1. Synthesis and characterization of metal aryl isocyanide complexes

2.1.1. Synthesis and characterization of $Cp^*M(CNAr)Cl_2$ complexes

The dichloro complexes are easily produced starting from the rhodium or iridium bridging halide dimers (**1** or **2**) in combination

* Corresponding author. Tel.: +1 585 275 5493.
E-mail address: jones@chem.rochester.edu (W.D. Jones).

0020-1693/$ - see front matter © 2013 Elsevier B.V. All rights reserved.
http://dx.doi.org/10.1016/j.ica.2013.07.039

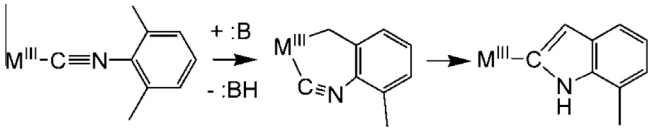

Fig. 1. Proposed tandem electrophilic C–H activation/cyclization.

with a stoichiometric amount of aryl isocyanide producing bench stable, monomeric $Cp^*M(CNAr)Cl_2$ [Ar = xylyl or 2,6-diethylphenyl (′)] in good to excellent yields similar to previously reported syntheses (Eq. (1)) [42–44].

$$[Cp^*MCl_2]_2 + 2\ \text{eqv. CNAr} \rightarrow Cp^*M(CNAr)Cl_2 \quad (1)$$

The crude products are typically orange for iridium complexes and red for the corresponding rhodium complexes. NMR and IR spectral data for these complexes are summarized in Table 1. Some features are worth pointing out in the spectra. First, the shift for the Cp^* resonance depends on the combination of the metal and the halogen while the resonances for the isocyanide are largely unaffected by either. Second, in the $^{13}C\{^1H\}$ spectra, the isocyanide carbon bound to the metal is difficult to observe due to coupling to the quadrupolar nitrogen and the metal center. The ipso carbon of the isocyanide which is also coupled to nitrogen is also not observed. The IR spectra of these complexes are typical in that the C≡N stretching frequency appears in the range 2100–2200 cm^{-1}. The C≡N stretching frequencies are of lower energy in the iridium complexes in comparison to the rhodium analogs overall, but the energy is greater than observed in the free isocyanide (2120 cm^{-1}), implying little π-backbonding upon coordination to either metal.

2.1.2. Synthesis and characterization of $Cp^*M(CNAr)I_2$ complexes

The diiodo complexes are made via halide metathesis in refluxing THF in the presence of a 10-fold excess of sodium iodide. While the dichloro complexes are not entirely soluble in THF, once the sodium iodide is added the color darkens, more prominently for rhodium complexes than iridium. Rhodium complexes become dark maroon, while the iridium complexes are a darker orange (Eq. (2)).

$$Cp^*M(CNAr)Cl_2 + 2\ \text{eqv. NaI} \rightarrow Cp^*M(CNAr)Cl_2 + 2\ \text{eqv.NaCl} \quad (2)$$

Both the IR and ^1H NMR spectra of the diiodo complexes are similar to the dichloro complexes but the Cp^* methyl resonances become more de-shielded and the stretching frequencies of the C≡N bond become lower in energy (Table 1). In some cases NMR spectral analysis of the product from the metathesis reactions shows the presence of another Cp^* peak that corresponds to the iodo version of the starting dichloro-dimer. This can be circumvented by first performing the iodide metathesis on **1** or **2** under the same conditions to obtain the $[Cp^*MI_2]_2$ compound. The diiodo-dimer can then be cleaved by addition of an isocyanide yielding the same diiodo complexes.

2.1.3. Synthesis and characterization of (p-cymene)Ru(CNAr)Cl_2 complexes

By simple extension to the group 9 complexes the *p*-cymene ruthenium complexes were made accordingly by adding a stoichiometric amount of aryl isocyanide to a solution of $[(p\text{-cymene})RuCl_2]_2$ (**3**) in dichloromethane (Eq. (4), X = Cl). Several modifications to the synthesis of the ruthenium complexes were necessary. Reactions performed under identical conditions to the group 9 complexes gave low yields. The solubility of **3** in THF is poor, as is the solubility of the isocyanide complexes. CH_2Cl_2 proved to be a better solvent for the reaction, and the reaction times were greatly extended to ensure complete coordination of the isocyanide. ^1H NMR and IR spectral data for these complexes are summarized in Table 2.

As noted previously with the group 9 complexes, the changes in the spectral data for the ruthenium complexes behave similarly. The *p*-cymene resonances are affected by the halogen bound to the metal and the effect on the isocyanide is more noticeable via IR than by ^1H NMR spectroscopy. For the ruthenium complexes bearing the 2,6-xylyl isocyanide, the C≡N stretching frequency appears in between that of the analogous iridium and rhodium complexes. However, when looking at the complexes bearing 2,6-diethylphenyl isocyanide, the C≡N stretching frequency is lower in energy than in the iridium complexes.

2.1.4. Synthesis and characterization of (p-cymene)Ru(CNAr)I_2 and alternative synthesis of $[(p\text{-cymene})RuI_2]$

The halide metathesis used for the group 9 complexes can extended to include the analogous ruthenium complexes. Similar problems arose where the $[(p\text{-cymene})RuI_2]_2$ dimer (**3′**) would form under prolonged reaction times. Since all of the complexes have similar solubility, purification of the complexes after synthesis is not straightforward. Rather, it is more feasible for the ruthenium complexes to synthesize them via isocyanide-induced cleavage of **3′** (Eqs. (3) and (4)) [45–48]. The reaction time for the diiodo analogs was greatly extended to ensure complete coordination of the isocyanide. Characterization of these compounds was straightforward, with the *p*-cymene resonances being slightly de-shielded in comparison to the dichloro compounds. More notably, the IR for these compounds shows that the C≡N stretch of the 2,6-xylyl isocyanide is between that of the corresponding iridium and rhodium complexes, but for 2,6-diethylphenyl isocyanide the C≡N stretch is lower in energy than the in related iridium compound.

Table 1
^1H NMR and IR spectral data for complexes **1a**, **1b**; **2a**, **2b**; **1a′**, **1b′**; **2a′**, **1b′**.

Complex	^1H NMR resonances,[a] δ		IR[c] (solid), cm^{-1}
	Cp^*	CNAr	
Cp^*IrCl_2(CN-2,6-Xyl) (**1a**)	1.86 (s)	7.16 (m, 1H)7.09 (d, 2H)2.45 (s, 6H)	2154
Cp^*RhCl_2(CN-2,6-Xyl)[b] (**2a**)	1.85 (s)	7.2 (m, 1H)7.1 (d, 2H)2.47 (s, 6H)	2172[d]
Cp^*IrI_2(CN-2,6-Xyl)[b] (**1b**)	2.14 (s)	7.12 (m, 3H)2.5 (s, 6H)	2133[d]
Cp^*RhI_2(CN-2,6-Xyl)[b] (**2b**)	2.17 (s)	7.16 (m, 1H)7.08 (d, 2H)2.5 (s, 6H)	2150[d]
Cp^*IrCl_2(CN-2,6-$Et_2C_6H_3$) (**1a′**)	1.85 (s)	7.24 (m, 1H)7.11 (d, 2H)2.82 (q, *J* = 7.6, 7.2 Hz, 4H)1.26 (t, *J* = 7.6 Hz, 6H)	2158
Cp^*RhCl_2(CN-2,6- $Et_2C_6H_3$) (**2a′**)	1.84 (s)	7.28 (m, 1H)7.12 (d, 2H)2.84 (q, *J* = 7.6, 7.2 Hz, 4H)1.27 (t, *J* = 7.6 Hz, 6H)	2173
Cp^*IrI_2(CN-2,6- $Et_2C_6H_3$)(**1b′**)	2.14 (s)	7.21 (m, 1H)7.12 (d, 2H)2.87 (q, *J* = 7.6, 7.2 Hz, 4H)1.27 (t, *J* = 7.6 Hz, 6H)	2150
Cp^*RhI_2(CN-2,6- $Et_2C_6H_3$)(**2b′**)	2.16 (s)	7.23 (m, 1H)7.1 (d, 2H)2.86 (q, *J* = 7.6, 7.2 Hz, 4H)1.27 (t, *J* = 7.6 Hz, 6H)	2163

[a] $CDCl_3$ solvent, 25 °C.
[b] Previously reported in C_6D_6.
[c] Reference values (ATR): 2,6-xylyl isocyanide, 2120 cm^{-1}; 2,6-diethylphenyl isocyanide, 2114 cm^{-1}.
[d] Previously reported in KBr pellet.

Table 2
^{1}H NMR and IR spectral data for complexes **3a**, **3b**; **3a′**, **3b′**.

Complex	^{1}H NMR resonances,[a] δ		IR (solid), cm^{-1}
	p-cymene	CNAr	
(*p*-cymene)$RuCl_2$(CN-2,6-Xyl) (**3a**)	5.69 (d, *J* = 6 Hz, 2H)5.52 (d, *J* = 6 Hz, 2H)2.91 (sept, *J* = 6.8 Hz, 1H)2.33 (s, 3H)1.31 (d, *J* = 6.8 Hz, 6H)	7.15 (m, 1H)7.07 (d, 2H)2.45(s, 6H)	2164
(*p*-cymene)RuI_2(CN-2,6-Xyl) (**3b**)	5.74 (d, *J* = 6 Hz, 2H)5.6 (d, *J* = 6 Hz, 2H)3.06 (sept, *J* = 6.8 Hz, 1H)2.61 (s, 3H)1.32 (d, *J* = 6.8 Hz, 6H)	7.11 (m, 1H)7.06 (d, 2H)2.51 (s, 6H)	2144
(*p*-cymene)$RuCl_2$ (CN-2,6- $Et_2C_6H_3$) (**3a′**)	5.69 (d, *J* = 6 Hz, 2H)5.52 (d, *J* = 6 Hz, 2H)2.93 (sept, *J* = 6.8 Hz, 1H)2.33 (s, 3H)1.32 (d, *J* = 6.8 Hz, 6H)	7.25 (m, 1H)7.11 (d, 2H)2.84 (q, *J* = 7.6, 7.2 Hz, 4H)1.32 (t, *J* = 7.6 Hz, 6H)	2154
(*p*-cymene)RuI_2(CN-2,6- $Et_2C_6H_3$)(**3b′**)	5.74 (d, *J* = 6 Hz, 2H)5.6 (d, *J* = 6 Hz, 2H)3.08 (sept, *J* = 6.8 Hz, 1H)2.6 (s, 3H)1.32 (d, *J* = 6.8 Hz, 6H)	7.2 (m, 1H)7.1 (d, 2H)2.88 (q, *J* = 7.6, 7.2 Hz, 4H)1.27 (t, *J* = 7.6 Hz, 6H)	2141

[a] $CDCl_3$ solvent, 25 °C.

Table 3
^{1}H NMR and IR spectral data for cationic solvent complexes of **1a**, **1b**, **1a′**, **1b′**.

Complex	^{1}H NMR resonances,[a,b] δ		IR[c] (solid), cm^{-1}
	Cp*	CNAr	
[Cp*IrCl(MeCN)(CN-2,6-Xyl)]PF_6 (**1a[PF$_6$]**)	1.88 (s)	7.34 (m, 1H)7.27 (d, 2H)2.45(s, 6H)	2327, 2185
[Cp*IrI(MeCN)(CN-2,6-Xyl)]PF_6 (**1b[PF$_6$]**)	2.04 (s)	7.32 (m, 1H)7.26 (d, 2H)2.48 (s, 6H)	2324, 2176
[Cp*IrCl(MeCN)(CN-2,6- $Et_2C_6H_3$)]PF_6(**1a′[PF$_6$]**)	1.89 (s)	7.42 (m, 1H)7.29 (d, 2H)2.82 (q, *J* = 7.6, 7.2 Hz, 4H)1.26 (t, *J* = 7.6 Hz, 6H)	2332, 2183
[Cp*IrI(MeCN)(CN-2,6- $Et_2C_6H_3$)]PF_6(**1b′[PF$_6$]**)	2.04 (s)	7.39 (m, 1H)7.28 (d, 2H)2.85 (q, *J* = 7.6, 7.2 Hz, 4H)1.26 (t, *J* = 7.6 Hz, 6H)	2331, 2175
[Cp*RhI(MeCN)(CN-2,6-Xyl)]PF_6 (**2b[PF$_6$]**)	2.02 (s)	7.34 (t, 1H)7.28 (d, 2H)2.48(s, 6H)	2326, 2182

[a] CD_3CN solvent, 25 °C.
[b] Methyl peak for coordinated acetonitrile is δ 1.96 for each complex.
[c] Reference value (ATR): acetonitrile, 2253 cm^{-1}.

$$[(p\text{-cymene})RuCl_2]_2 + 4\ \text{eqv. NaI} \rightarrow [(p\text{-cymene})RuCl_2]_2 + 4\ \text{eqv. NaCl} \quad (3)$$

$$[(p\text{-cymene})RuCl_2]_2 + 2\ \text{eqv. CNAr} \rightarrow 2\ \text{eqv.}(p\text{-cymene})Ru(CNAr)I_2 \quad (4)$$

2.2. Synthesis and characterization of cationic metal acetonitrile complexes

Attempts to induce C–H activation/cyclization were first made with silver acetate to abstract the halogen from a complex and generate the open site necessary for acetate-assisted C–H activation. While halogen abstraction occurred readily, C–H activation was not observed (vida infra). Isolation of the intermediate cationic species proved unfeasible with acetate as a counter-ion, but exchange for a bulky counter-ion such as hexafluorophosphate allowed for isolation and crystallization. Slow addition of a solution of $AgPF_6$ in dry acetonitrile to a solution of the neutral dihalo complex in dry acetonitrile under an atmosphere of nitrogen produces the solvent trapped cationic metal complex in moderate to good yields. Precipitation of the product occurs upon adding excess diethyl ether to a concentrated solution following filtration of the silver halide by-product. ^{1}H NMR and IR spectral data for these complexes are summarized in Table 3.

Interestingly, in the iridium and rhodium iodo-solvent complexes, the Cp* resonances are significantly more shielded upon removing the halide and coordinating an acetonitrile molecule. As stated previously the carbene carbon of the isocyanide is unobservable in the $^{13}C\{^1H\}$ NMR spectrum and the nitrile carbon of acetonitrile is also not observed for similar reasons. The ν(C≡N) stretching frequencies are particularly more affected by the halide abstraction than are the changes in chemical shifts in the NMR spectra. Each complex shows an increase in energy for the C≡N bond stretch of about 30 cm^{-1} while the stretch corresponding to the acetonitrile bond is relatively unchanged in all of the complexes. The analogous rhodium and ruthenium mono-chlorides were never isolated. The rhodium chloride compounds subjected to these conditions were unstable in solution and disproportioned faster than crystallizing. On a few occasions a new rhodium dimer was isolated and characterized as $[Cp^*RhCl(MeCN)]_2[PF_6]_2$ (**4**) but no $[Cp^*RhCl(CNAr)_2]PF_6$ was ever isolated. Ruthenium compounds, other than **3b[PF$_6$]**, were never isolated as solids and crystallization of this ruthenium complex required several days at −30 °C. The long crystallization period was also seen for the rhodium iodo-solvent complex, **2b′[PF$_6$]**, but attempts to isolate the target molecule resulted in isolation of either $[Cp^*Rh(MeCN)_3,PF_6]_2$ (**5**), which was characterized by X-ray diffraction, or the starting material, **2b′** [49]. Even though isocyanides are strong σ-donor ligands they are labile, and this observation could be extended to the ruthenium complexes as well as their isolations and/or crystallizations were not routine.

2.3. X-ray crystallography

2.3.1. Neutral complexes

X-ray quality crystals for neutral complexes were grown, typically, by vapor diffusion of pentane into a concentrated solution of either dichloromethane or chloroform. Decent crystals could also be grown by simple evaporation of the solution overnight. The observed water and oxygen stability allows for several crystallization methods utilizing readily accessible solvents. Table 4 describes selected bonds and angles and Table 7 describes selected parameters of the X-ray diffraction experiments.

All structures obtained are tetrahedral-like 'piano-stools' and similar to each other in most aspects as seen in Table 4. The geometrical variations are statistically insignificant. The isocyanide bond length is nearly unaffected upon coordination of M^{3+} center in comparison to the free isocyanide (1.161 Å) [50], consistent with minimal π-back bonding and the isocyanide acting purely as a σ-donor. However, **1a** does have a significant amount of C–N–Ar bending (168°), comparable to that seen in the previously reported **1b** (166°). **2b** is isostructural and has a C≡N–Ar angle of ~167°.[1]

[1] An isomorph was crystallized via layering hexane on a concentrated solution in DCM: *a* = 8.689(3) Å, *b* = 31.360(9) Å, *c* = 22.961(7) Å; α = 90°, β = 97.216(4)°, γ = 90°. The full report is in the SI.

Table 4
Selected distances and angles for neutral complexes.

Compound	C≡N length (Å)	M–CN length (Å)	M–C≡N angle (°)	C≡N-Ar angle (°)	Ave. π-stacking distance (Å)
1a	1.157(3)	1.932(3)	176.0(2)	168.4(3)	3.74–3.86[a]
1a′	1.154(4)	1.923(3)	177.3(3)	177.0(4)	3.50–3.63[a]
1b′	1.161(3)	1.913(3)	176.4(2)	172.2(3)	3.37–3.39
2a	1.1582(18)	1.9675(14)	173.86(12)	170.07(14)	3.74–3.88[a]
2b	1.161(2)	1.9385(18)	179.03(16)	166.96(18)	-
2a′	1.1562(17)	1.9582(13)	174.97(12)	173.71(14)	-
2b′	1.160(2)	1.9340(18)	177.46(16)	173.59(18)	3.30–3.37
3a	1.155(2)	1.9617(19)	177.77(17)	176.8(2)	3.45–3.53
3b	1.161(3)	1.942(2)	176.69(19)	177.2(2)	3.62–3.75
3a′	1.159(3)	1.952(2)	175.55(18)	171.9(2)	3.37–3.45
3b′	1.162(4)	1.940(3)	178.1(3)	173.5(3)	3.47–3.49

[a] Average distance for T-stacking of Cp* methyl to isocyanide arene ring of adjacent molecule.

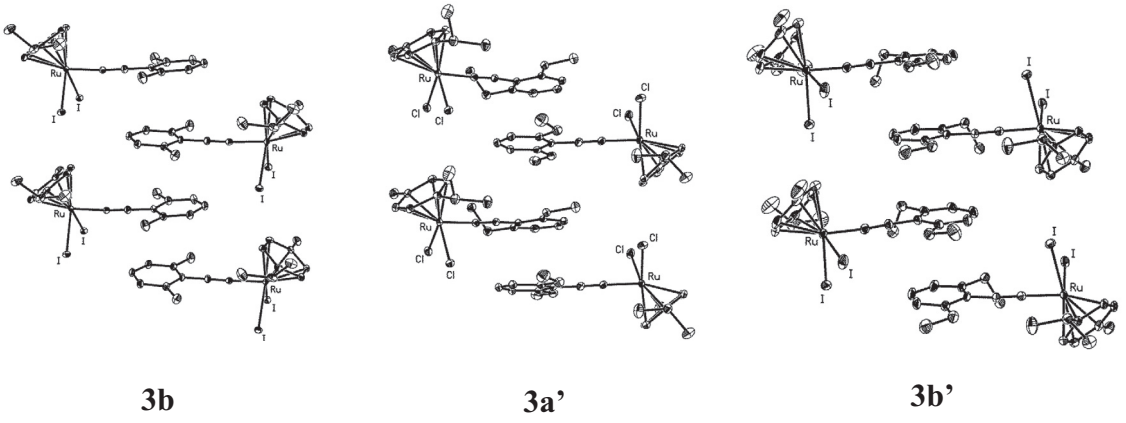

Fig. 2. Intermolecular π-stacking displayed in the crystal structures of **3a′**, **3b**, and **3b′**. Thermal ellipsoids are drawn at the 50% probability level. The asymmetric unit's displayed are doubled. Hydrogen atoms were removed for clarity.

Table 5
Selected distances and angles for cationic complexes of isocyanide.

Compound	C≡N length (Å)	M–CN length (Å)	M–C≡N angle (°)	C≡N-Ar angle (°)	Ave. π-stacking distance (Å)
1a[PF$_6$]	1.150(3)	1.955(3)	178.6(2)	175.9(3)	3.44–3.45
1b[PF$_6$]	1.158(3)	1.952(2)	179.5(2)	175.4(2)	3.47–3.48
1a′[PF$_6$]	1.156(6)	1.955(5)	177.5(5)	175.2(5)	3.42–3.43
1b′[PF$_6$]	1.163(5)	1.958(4)	176.8(4)	174.9(5)	3.51–3.52
2b[PF$_6$]	1.158(4)	1.975(3)	179.7(3)	175.9(3)	3.50–3.51

Table 6
Selected distances and angles for cationic complexes of acetonitrile.

Compound	MeC≡N length (Å)	M–NCMe length (Å)	M–N≡CMe angle (°)	N≡C–Me angle (°)
1a[PF$_6$]	1.139(3)	2.063(2)	168.4(2)	179.0(3)
1b[PF$_6$]	1.137(3)	2.058(2)	168.5(2)	178.0(3)
1a′[PF$_6$]	1.138(5)	2.050(3)	171.3(3)	178.6(5)
1b′[PF$_6$]	1.135(5)	2.052(3)	173.1(3)	179.5(5)
2b[PF$_6$]	1.135(5)	2.084(3)	169.0(3)	177.5(4)

The analogous ruthenium compound **3a** is unique in comparison to the group 9 compounds with a space group of $P2_1/n$ while **1a** and **2a** are $C2/c$. While most of the complexes have only one molecule in the asymmetric unit, complexes **3b**, **3a′**, and **3b′** have two independent molecules in the asymmetric unit (Fig. 2). Other than compounds **1a**, **1a′**, **2a**, **2a′**, and **2b**, many of the structures display characteristic π-stacking within a commonly accepted range of 3.3–3.8 Å [51]. The measured distance ranges can be seen in Table 4. Structures **1a**, **1a′**, and **2a** exhibit T-stacking between a methyl group from a coordinated Cp* to the arene ring of an isocyanide on an adjacent molecule. Otherwise, all rhodium structures were isostructural with the analogous iridium structures. The ruthenium structures were unique from the group 9 complexes and also from each other. **3a** packed in a $P2_1/n$ space group and had only one molecule in the asymmetric unit. The other 3 ruthenium structures, **3b**, **3a′**, and **3b′**, which had crystallized in the $P\bar{1}$ space group, are not isostructural to **3a**.

2.3.2. Cationic complexes

Crystallization of these cationic complexes was also done via vapor diffusion of diethyl ether into a concentrated solution of the crude material in acetonitrile. The 2,6-xylylisocyanide coordinated complexes would crystallize overnight at room temperature under a nitrogen atmosphere while the 2,6-diethyphenyl isocyanide complexes took several days at −30° to crystallize. Structural analysis of these cationic complexes shown that the C≡N–Ar angle became more linear compared to the neutral precursors. Table 5 shows selected bond lengths and angles for the cationic complexes for the isocyanide ligand and Table 6 shows structural information for the acetonitrile ligand. These complexes can be considered 'chiral-at-metal' as there are four distinct ligands attached to one metal center that is of tetrahedral geometry. However, all of these cationic compounds crystallized in the centrosymmetric space group $P\bar{1}$ as a pair of enantiomers. All of the cationic complexes crystallized display characteristic π-stacking and the measured

Table 7
Summary of crystallographic data for complexes.

Parameter	**3b**	**3a′**	**3b′**	**1a[PF$_6$]**	**1b[PF$_6$]**	**1a′[PF$_6$]**	**1b′[PF$_6$]**	**2b[PF$_6$]**
Empirical formula	$C_{19}H_{23}I_2NRu$	$C_{21}H_{27}Cl_2NRu$	$C_{21}H_{27}I_2NRu$	$C_{21}H_{27}ClF_6IrN_2P$	$C_{21}H_{27}F_6IIrN_2P$	$C_{23}H_{31}ClF_6IrN_2P$	$C_{23}H_{31}F_6IIrN_2P$	$C_{21}H_{27}F_6IN_2PRh$
Formula weight	620.25	465.41	648.30	680.06	771.51	708.12	799.57	682.22
Crystal System	triclinic	triclinic	triclinic	triclinic	triclinic	triclinic	triclinic	triclinic
Space group	$P\bar{1}$	$P\bar{1}$	$P\bar{1}$	$P\bar{1}$	$P\bar{1}$	$P\bar{1}$	$P\bar{1}$	$P\bar{1}$
a (Å)	7.4768(6)	7.2867(3)	7.6913(6)	7.815(3)	7.9835(8)	7.7315(8)	7.9155(12)	7.9489(8)
b (Å)	15.7980(12)	13.9017(7)	13.3242(11)	9.298(3)	9.3302(9)	10.9322(12)	11.2196(16)	9.2454(9)
c (Å)	17.9638(14)	20.7264(10)	24.663(2)	16.848(6)	16.9294(16)	15.3788(16)	15.399(2)	17.2120(17)
α (°)	72.7420(10)	77.084(1)	75.408(2)	88.007(7)	86.656(2)	88.062(2)	88.1993(3)	87.143(2)
β (°)	84.997(2)	86.611(1)	85.356(2)	81.362(7)	80.435(2)	89.430(2)	88.406(3)	80.231(2)
γ (°)	89.865(2)	82.908(1)	78.374(2)	81.701(7)	79.976(2)	79.906(2)	77.583(3)	81.291(2)
V(Å^3)	2018.0(3)	2029.68(16)	2223.9(4)	1197.6(8)	1224.0(2)	1279.0(2)	1334.63	1224.0(2)
Z	4	4	4	2	2	2	2	2
D_{calc} (Mg/m^3)	2.042	1.523	1.798	1.886	2.093	1.839	1.990	1.839
Goodness-of-fit, F^2	1.035	1.021	1.034	1.061	1.051	1.014	1.060	1.013
Final R indices	R_1 = 0.0310	R_1 = 0.0437	R_1 = 0.0379	R_1 = 0.0344	R_1 = 0.0306	R_1 = 0.0504	R_1 = 0.0448	R_1 = 0.0486
[$I > 2\sigma(I)$]	wR_2 = 0.0651	wR_2 = 0.0819	wR_2 = 0.0781	wR_2 = 0.0656	wR_2 = 0.0587	wR_2 = 0.0874	wR_2 = 0.1058	wR_2 = 0.0941
R indices	R_1 = 0.0437	R_1 = 0.0691	R_1 = 0.0537	R_1 = 0.0481	R_1 = 0.0425	R_1 = 0.0879	R_1 = 0.0724	R_1 = 0.0930
(all data)	wR_2 = 0.0697	wR_2 = 0.0913	wR_2 = 0.0830	wR_2 = 0.0694	wR_2 = 0.0621	wR_2 = 0.1030	wR_2 = 0.1201	wR_2 = 0.01085
Parameter	**1a**	**2a**	**3a**	**1a′**	**1b′**	**2a′**	**2b′**	**2b**
Empirical formula	$C_{19}H_{24}Cl_2IrN$	$C_{19}H_{24}Cl_2NRh$	$C_{20}H_{25}Cl_4NRu$	$C_{21}H_{28}Cl_2IrN$	$C_{21}H_{28}I_2IrN$	$C_{21}H_{28}Cl_2NRh$	$C_{21}H_{28}I_2NRh$	$C_{19}H_{24}I_2NRh$
Formula weight	529.49	440.20	522.28	557.54	740.44	468.25	651.15	623.10
Crystal System	monoclinic	monoclinic	monoclinic	monoclinic	monoclinic	monoclinic	monoclinic	monoclinic
Space group	$C2/c$	$C2/c$	$P2_1/n$	$P2_1/c$	$P2_1/c$	$P2_1/c$	$P2_1/c$	$P2_1/c$
a (Å)	22.932(2)	22.8732(16)	17.2637(13)	8.3293(9)	16.5408(17)	15.452(2)	16.528(2)	11.1943(11)
b (Å)	13.9600(15)	14.0280(10)	7.1016(5)	14.9714(16)	8.9938(9)	8.3872(11)	9.0176(11)	8.3141(8)
c (Å)	14.3440(15)	14.2045(10)	19.6517(15)	16.6103(18)	15.8158(16)	16.535(2)	15.7935(19)	21.985(2)
α (°)	90	90	90	90	90	90	90	90
β (°)	125.002(2)	124.867(1)	115.943(1)	91.268(2)	109.055(2)	101.271(2)	108.939(2)	97.148(2)
γ (°)	90	90	90	90	90	90	90	90
V(Å^3)	3761.4(7)	3739.5(5)	2166.6(3)	2070.8(4)	2223.9(4)	2101.6(5)	2226.5(5)	2030.2(3)
Z	8	8	4	4	4	4	4	4
D_{calc} (Mg/m^3)	1.870	1.564	1.601	1.788	2.211	1.480	1.943	2.039
Goodness-of-fit, F^2	1.024	1.029	1.034	1.091	1.051	1.032	1.048	1.099
Final R indices	R_1 = 0.0296	R_1 = 0.0297	R_1 = 0.0409	R_1 = 0.0388	R_1 = 0.0305	R_1 = 0.0309	R_1 = 0.0293	R_1 = 0.0278
[$I > 2\sigma(I)$]	wR_2 = 0.0613	wR_2 = 0.0669	wR_2 = 0.0978	wR_2 = 0.0840	wR_2 = 0.0671	wR_2 = 0.0632	wR_2 = 0.0578	wR_2 = 0.0556
R indices	R_1 = 0.0459	R_1 = 0.0451	R_1 = 0.0606	R_1 = 0.0515	R_1 = 0.0407	R_1 = 0.0472	R_1 = 0.0429	R_1 = 0.0372
(all data)	wR_2 = 0.0672	wR_2 = 0.0723	wR_2 = 0.1069	wR_2 = 0.0882	wR_2 = 0.0711	wR_2 = 0.0696	wR_2 = 0.0625	wR_2 = 0.00581

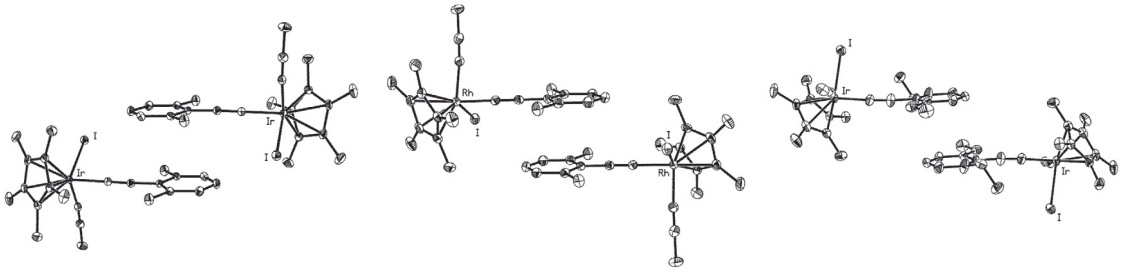

Fig. 3. Intermolecular π-stacking displayed in the crystal structures of **1b[PF$_6$]**, **2b[PF$_6$]**, and **1b′[PF$_6$]**. Thermal ellipsoids are drawn at the 50% probability level. The asymmetric units displayed are double. Hydrogen atoms were removed for clarity.

distance ranges are in Table 5. A few examples are shown in Fig. 3 and show quite similar structures but are not isostructural.

2.4. Halogen abstraction tandem cyclometallation via electrophilic C–H activation attempts

2.4.1. Reactions with bases

The C–H activation of phenyl imines and phenyl pyridines under mild conditions using **1** or **2** with sodium acetate was previously shown by our group [26,27]. Applying the same conditions to either **1a** or **2a** shown no C–H activation of the benzylic sp^3 hydrogens though the chloride had been displaced by acetate. Also letting any dimer, **1**, **2**, or **3**, react with sodium acetate first and then adding the 2,6-xylylisocyanide to the intermediate metal-acetate complex only generated the corresponding isocyanide complex. Using potassium carbonate shown loss of the isocyanide and complete decomposition of **2a**. Stronger nucleophilic bases such as sodium phenolate and potassium *t*-butoxide decomposed **2a** quickly.

2.4.2. Reactions with silver salts

Attempts with sodium acetate seemed inconclusive and the extension to silver acetate was made to completely remove the halogen since with sodium acetate and a dimer like **2** could be in

equilibrium with $Cp^*MCl(OAc)$ and $Cp^*M(OAc)_2$. The formation of silver chloride would drive to equilibrium to favor the $Cp^*M(OAc)_2$ [27] While adding silver acetate, either stoichiometricly or in excess, did remove the halogen no C–H activation was observed and isolation of an intermediate metal–isocyano–acetate complex was not accomplished. Other silver salts such as silver triflate and silver hexafluorophosphate were used to generate those intermediates as seen above. In regards to C–H activation neither the PF_6^- nor the OTf^- anions were helpful and no cationic complexes with triflate as the counterion were ever isolated. Heating either **1a** or **2a** with silver acetate or silver trifluoroacetate also did not promote the formation of an indole species and none were detected via ^1H NMR spectroscopy. Heating **1a** or **3a** with silver triflate also proved futile for generating coordinatively unsaturated species.

2.4.3. Thermolysis and protonolysis

The chloro analogues of the 2,6-xylylisocyanide complexes were heated in benzene but no indole intermediates were detected. The ruthenium lost *p*-cymene and no reaction was observed for the group 9 complexes. Heating **2a** in trifluoroacetic acid-d_1 only caused the isocyanide to dissociate.

3. Conclusions

Several new ruthenium, rhodium, and iridium complexes were synthesized and structurally characterized and analyzed. Halide abstraction with bulky silver salts allowed for the isolation of several 'chiral-at-metal' cationic iridium and rhodium complexes. However further reaction of these complexes to achieve C–H activation was not observed at the benzylic carbon of the isocyanide, as supported by crystal structure determination of the cationic solvent adducts.

4. Experimental

4.1. General procedures, materials and instrumentation

THF, CH_2Cl_2, and diethyl ether were purified by passage through activated alumina columns in a Innovative Technology, Inc. PS-MD-6 solvent purification system. Once reactions were completed, however, subsequent workups were done without precaution, as the neutral compounds are bench stable. Acetonitrile was purified through activated alumina and Q5 columns from Glass Contour Co. Pentane, Celite®, and sodium iodide (Fischer Scientific) were used as received. Manipulations for synthesis of the cationic complexes were performed under nitrogen in a M. Braun glove box with oxygen and water levels below 1 ppm. Glassware used in the glove box was dried at 150 °C overnight. Silver hexafluorophosphate was purchased from Strem Chemicals Inc. and used under nitrogen. Deuterated solvents were purchased from Cambridge Isotope Laboratories. Chloroform-d_1 (δ 7.26) was used as received and acetonitrile-d_3 (δ 1.94) was dried over CaH_2 and distilled under vacuum. 2,6-Xylyl isocyanide was either purchased from Strem Chemicals Inc. or synthesized by a modified published procedure [52]. 2,6-Diethylphenyl isocyanide was synthesized by previously reported procedure [53]. ^1H NMR spectra were recorded using a Avance 400 MHz spectrometer and $^{13}C\{^1H\}$ NMR spectra were recorded using an Avance 500 MHz spectrometer. Elemental analyses were obtained from theCENTC Elemental Analysis Facility at the University of Rochester. IR spectra were recorded using a Shimadzu IR Prestige-21 FTIR spectrophotometer with a PIKE Technologies MIRacle™ single reflection ATR. X-ray diffraction data were collected using a Bruker SMART APEX II CCD Platform diffractometer.

4.2. Synthesis of Cp^*IrCl_2(CN-2,6-Xyl), ***1a***

2,6-Xylyl isocyanide (83 mg, 0.633 mmol) is added to a solution of $[Cp^*IrCl_2]_2$ (26.2 mg, 0.330 mmol) in THF. The reaction is sealed and allowed to stir for 1 h. Then the solvent is evaporated, pentane is added, the mixture is sonicated and then filtered through a frit to remove excess isocyanide; crude yield 80%. The crude material was re-crystallized via vapor diffusion with CH_2Cl_2/pentane; purified yield 72%. ^1H NMR (400 MHz, $CDCl_3$): δ 7.16 (m, 1H), 7.09 (d, 2H), 2.45 (s, 6H), 1.86 (s, 15H) $^{13}C\{^1H\}$ NMR (125 MHz, $CDCl_3$): δ 135.5, 132.4, 129.1, 127.9, 127.3, 18.9, 9.2. IR (solid) 2154 cm^{-1}. *Anal.* Calc. for $C_{19}H_{24}Cl_2IrN$: C, 43.09; H, 4.56; N, 2.64. Found: C, 43.07; H, 4.49; N, 2.71%.

4.3. Synthesis of Cp^*RhCl_2(CN-2,6-Xyl), ***2a***

The synthesis is analogous to **1a**; crude yield 98%. *Anal.* Calc. for $C_{19}H_{24}Cl_2NRh$: C, 51.83; H, 5.49; N, 3.18. Found: C, 51.76; H, 5.41; N, 3.14%.

4.4. Synthesis of Cp^*IrI_2(CN-2,6-Xyl), ***1b***

The synthesis is analogous to **1b′**; crude yield 84%. *Anal.* Calc. for $C_{19}H_{24}I_2IrN$: C, 32.03; H, 3.39; N, 1.96. Found: C, 31.60; H, 3.27; N, 1.93%.

4.5. Synthesis of Cp^*RhI_2(CN-2,6-Xyl), ***2b***

The synthesis is analogous to **1b′**; crude yield 99%. *Anal.* Calc. for $C_{19}H_{24}I_2NRh$: C, 36.62; H, 3.88; N, 2.24. Found: C, 36.34; H, 3.75; N, 2.22%.

4.6. Synthesis of $[(p\text{-cymene})RuI_2]_2$, ***'3'***

$[(p\text{-cymene})RuCl_2]_2$ (171 mg, 0.279 mmol) and NaI (210 mg, 1.40 mmol) are added to a round bottom flask with a stir bar followed by 20 mL THF. A reflux condenser is attached and the flask is submerged in an oil bath and refluxed for 2 h. Then the mixture is allowed to cool to room temperature and the solvent is evaporated. The residue is extracted with CH_2Cl_2, sonicated, and filtered through Celite with CH_2Cl_2. The process is repeated 3 times to remove any sodium halide. The solvent is evaporated from the combined extracts; crude yield 99%. *Anal.* Calc. for $C_{20}H_{28}I_4Ru_2$: C, 24.55; H, 2.88. Found: C, 24.54; H, 2.71%.

4.7. Synthesis of $(p\text{-cymene})RuCl_2$(CN-2,6-Xyl)·½CH_2Cl_2, ***3a***

2,6-Xylyl isocyanide (25.7 mg, 0.196 mmol) is added to a solution of $[(p\text{-cymene})RuCl_2]_2$ (60.8 mg, 0.0982 mmol) in dry CH_2Cl_2. The reaction is sealed and allowed to stir 2 h. The solvent is evaporated, pentane is added, the mixture is sonicated and then filtered through a frit and the process is repeated 3 times to remove excess isocyanide; crude yield 98%. The crude material was re-crystallized via vapor diffusion with CH_2Cl_2/pentane; purified yield 86%. ^1H NMR (400 MHz, $CDCl_3$): δ 7.15 (q, 1H), 7.07 (d, 2H), 5.69 (d, 2H), 5.52 (d, 2H), 5.28 (s, 1H), 2.91 (sept, 1H), 2.45 (s, 6H), 2.33 (s, 3H), 1.31 (d, 6H). $^{13}C\{^1H\}$ NMR (125 MHz, $CDCl_3$): δ 151.8, 135.7, 129.3, 128.0, 127.3, 108.4, 107.9, 88.9, 88.3, 53.6, 31.5, 22.7, 19.2, 19.1. IR (solid): 2164 cm^{-1}. *Anal.* Calc. for $C_{39}H_{48}Cl_6N_2Ru_2$: C, 48.81; H, 5.04; N, 2.91. Found: C, 48.81; H, 5.04; N, 2.90%.

4.8. Synthesis of $(p\text{-cymene})RuI_2$(CN-2,6-Xyl), ***3b***

2,6-Xylyl isocyanide (16.7 mg, 0.127 mmol) is added to a solution of **3** (61.4 mg, 0.0627 mmol) in dry CH_2Cl_2. The reaction is sealed and allowed to stir overnight. The solvent is evaporated,

pentane is added, then the mixture is sonicated and then filtered through a frit. The process is repeated 3 times to remove any sodium halide; crude yield 99%. The crude material was re-crystallized via vapor diffusion with CH_2Cl_2/pentane; purified yield 86%. ^{1}H NMR (400 MHz, $CDCl_3$): δ 7.11 (q, 1H), 7.06 (d, 2H), 5.74 (d, 2H), 5.60 (d, 2H), 3.06 (sept, 1H), 2.61 (s, 3H), 2.51 (s, 6H), 1.32 (d, 6H). ^{13}C{^{1}H} NMR (125 MHz, $CDCl_3$): δ 149.1, 135.9, 128.8, 128.0, 111.6, 107.1, 89.8, 89.0, 32.3, 23.1, 20.9, 19.5. IR (solid): 2144 cm^{-1}. *Anal.* Calc. for $C_{19}H_{23}I_2NRu$: C, 36.79; H, 3.73; N, 2.25. Found: C, 36.73; H, 3.50; N, 2.18%.

4.9. Synthesis of $Cp^*IrCl_2(CN\text{-}2,6\text{-}Et_2C_6H_3)\cdot CH_2Cl_2$, '**1a**'

$[Cp^*IrCl_2]_2$ (87.7 mg, 0.110 mmol) is added to a round bottom flask with a stir bar followed by 10 mL of THF. 2,6-Diethylphenylisocyanide (40.3 μL, 0.221 mmol) is added drop-wise while stirring. The flask is sealed and let stir for 1 h at room temperature. Then the solvent is evaporated and pentane is added and the mixture is sonicated and filtered. The process is repeated 3 time to remove any excess isocyanide; Crude yield 89%. The crude material was re-crystallized via vapor diffusion with CH_2Cl_2/pentane; purified yield 47%. ^{1}H NMR (400 MHz, $CDCl_3$):δ 7.24 (m, 1H), 7.11 (d, 2H), 5.28 (s, 2H) 2.82 (q, 4H), 1.85 (s, 15H), 1.26 (t, 6H). ^{13}C{^{1}H} NMR (125 MHz, $CDCl_3$): δ 141.6, 129.6, 126.4, 94.4, 86.3, 25.8, 14.2, 9.5, 9.3. IR (solid): 2158 cm^{-1}. *Anal.* Calc. for $C_{22}H_{30}Cl_4IrN$: C, 41.12; H, 4.70; N, 2.18. Found: C, 41.81; H, 4.67; N, 1.88%.

4.10. Synthesis of $Cp^*IrI_2(CN\text{-}2,6\text{-}Et_2C_6H_3)$, **1b**'

74.4 mg (0.133 mmol) of **1a**' and 201 mg (1.34 mmol) of NaI are added to a round bottom flask with a stir bar followed by 10 ml of THF. A reflux condenser is attached and the flask is submerged in an oil bath and refluxed for 3 h. Then the mixture is allowed to cool to room temperature and solvent is evaporated. The residue is extracted with CH_2Cl_2, sonicated, and filtered through Celite with CH_2Cl_2. The process was repeated 3 times to remove and sodium halide. The solvent is evaporated from the combined extracts; crude yield 95%. The crude material was re-crystallized via vapor diffusion with CH_2Cl_2/pentane; purified yield 98%. ^{1}H NMR (400 MHz, $CDCl_3$): δ 7.18 (m, 1H), 7.12 (d, 2H), 2.87 (q, 4H), 2.14 (s, 15H), 1.27 (t, 6H). ^{13}C{^{1}H} NMR (125 MHz, $CDCl_3$): δ 141.7, 129.1, 126.3, 95.3, 88.8, 25.7, 14.6, 10.7. IR (solid): 2150 cm^{-1}. *Anal.* Calc. for $C_{21}H_{28}Cl_4IrN$: C, 34.06; H, 3.81; N, 1.89. Found: C, 34.54; H, 3.80; N, 1.86%.

4.11. Synthesis of $Cp^*RhCl_2(CN\text{-}2,6\text{-}Et_2C_6H_3)$, **2a**'

The synthesis is analogous to **2a**; crude yield 95%, purified yield 89%. ^{1}H NMR (400 MHz, $CDCl_3$):δ 7.28 (t, 1H), 7.12 (d, 2H), 2.84 (q, 4H), 1.84 (s, 15H), 1.27 (t, 6H). ^{13}C{^{1}H} NMR (125 MHz, $CDCl_3$):δ 141.6, 130.0, 126.4, 125.4, 25.7, 14.1, 9.6. IR (solid): 2173 cm^{-1}. *Anal.* Calc. for $C_{21}H_{28}Cl_2NRh$: C, 53.86; H, 5.95; N, 2.98. Found: C, 53.75; H, 5.95; N, 2.98%.

4.12. Synthesis of $Cp^*RhI_2(CN\text{-}2,6\text{-}Et_2C_6H_3)$, **2b**'

The synthesis is analogous to **2b**; crude yield 99%, purified yield 92%. ^{1}H NMR (400 MHz, $CDCl_3$): δ 7.23 (t, 1H), 7.1 (d, 2H), 2.86 (q, 4H), 2.16 (s, 15H), 1.27 (t, 6H). ^{13}C{^{1}H} NMR (125 MHz, $CDCl_3$): δ 141.8, 129.6, 126.4, 125.8, 25.8, 14.7, 11.3. IR (solid): 2163 cm^{-1}. *Anal.* Calc. for $C_{21}H_{28}I_2NRh$: C, 38.73; H, 4.33; N, 2.15. Found: C, 38.57; H, 4.30; N, 2.08%.

4.13. Synthesis of $(p\text{-cymene})RuCl_2(CN\text{-}2,6\text{-}Et_2C_6H_3)$, **3a'**

The synthesis is analogous to **3a**; crude yield 99%, purified yield 90%. ^{1}H NMR (400 MHz, $CDCl_3$): δ 7.25 (m, 1H), 7.11 (d, 2H), 5.69 (d, 2H), 5.52 (d, 2H), 2.93 (septet, 1H), 2.84 (q, 4H), 2.33 (s, 3H), 1.32 (d, 6H), 1.27 (t, 6H). ^{13}C{^{1}H} NMR (125 MHz, $CDCl_3$): δ 141.5, 129.6, 108.4, 107.2, 88.7, 88.3, 31.4, 25.6, 22.5, 19.0, 14.2. IR (solid): 2154 cm^{-1}. *Anal.* Calc. for $C_{21}H_{27}Cl_2NRu$: C, 54.19; H, 5.84; N, 3.00. Found: C, 53.98; H, 5.77; N, 3.23%.

4.14. Synthesis of $(p\text{-cymene})RuI_2(CN\text{-}2,6\text{-}Et_2C_6H_3)$, **3b**'

The synthesis is analogous to **3b**; Crude yield 93%. Purified Yield 88%. ^{1}H NMR (400 MHz, $CDCl_3$): δ 7.2 (q, 1H), 7.1 (d, 2H), 5.74 (d, 2H), 5.6 (d, 2H), 3.08 (sept, 1H), 2.88 (q, 4H), 2.6 (s, 3H), 1.32 (d, 6H), 1.27 (t, 6H). ^{13}C{^{1}H} NMR (125 MHz, $CDCl_3$): δ 141.8, 129.3, 126.4, 111.7, 106.8, 89.7, 89.1, 32.3, 25.9, 23.1, 20.9, 14.9. IR (solid): 2141 cm^{-1}. *Anal.* Calc. for $C_{21}H_{27}I_2NRu$: C, 38.90; H, 4.19; N, 2.16. Found: C, 38.23; H, 4.09; N, 2.09%.

4.15. Synthesis of $[Cp^*IrCl(MeCN)(CN\text{-}2,6\text{-}Xyl)]PF_6$, **1a[PF$_6$]**

52.9 mg (0.0999 mmol) of **1** is added to a scintillation vial followed by a stir bar, and 10 mL of acetonitrile which is stirred vigorously. In a separate vial 25.5 mg (0.101 mmol) of $AgPF_6$ is dissolved in 2 mL of acetonitrile then added the solution drop-wise in 4 0.5 mL portions to the stirring mixture. The color immediately begins to lighten from goldenrod to lemon yellow and the reaction is stirred for 1 h. The stirring is stopped and the AgCl precipitate was allowed to settle before decanting and filtering through Celite with acetonitrile. The solution is concentrated, then precipitated with ether. The mixture is filtered on a frit and dried under vacuum; crude yield 88%. ^{1}H NMR (400 MHz, CD_3CN): δ 7.34 (q, 1H), 7.27 (d, 2H), 2.45 (s, 6H), 1.96 (s, 3H), 1.88 (s, 15H). ^{13}C{^{1}H} NMR (125 MHz, CD_3CN): δ 136.9, 131.2, 129.1, 97.8, 18.8, 9.4. IR (solid): 2327 cm^{-1} (M–N≡*C*-R), 2185 cm^{-1} (M-*C*≡*N*-Ar). *Anal.* Calc. for $C_{21}H_{27}ClF_6IrN_2P$: C, 37.08; H, 4.00; N, 4.11. Found: C, 37.17; H, 3.86; N, 4.17%.

4.16. Synthesis of $[Cp^*IrI(MeCN)(CN\text{-}2,6\text{-}Xyl)]PF_6$, **1b[PF$_6$]**

The synthesis is analogous to **1a[PF$_6$];** crude yield 87%. ^{1}H NMR (400 MHz, CD_3CN): δ 7.32 (q, 1H), 7.26 (d, 2H), 2.48 (s, 6H), 2.04 (s, 15H), 1.96 (s, 3H). ^{13}C{^{1}H} NMR (125 MHz, CD_3CN): δ 137.1, 131.1, 129.1, 98.5, 19.1, 10.3. IR (solid): 2324 cm^{-1} (M–N≡*C*-R), 2176 cm^{-1} (M-*C*≡*N*-Ar). *Anal.* Calc. for $C_{21}H_{27}F_6IIrN_2P$: C, 32.69; H, 3.52; N, 3.63. Found: C, 32.84; H, 3.35; N, 3.64%.

4.17. Synthesis of $[Cp^*IrCl(MeCN)(CN\text{-}2,6\text{-}EtC_6H_4)]PF_6$, **1a'[PF$_6$]**

The synthesis is analogous to **1a[PF$_6$]**; Yield 93%. ^{1}H NMR (400 MHz, CD_3CN): δ 7.42 (t, 1H), 7.29 (d, 2H), 2.82 (q, 4H), 1.96 (s, 3H), 1.89 (s, 15H), 1.26 (t, 6H). ^{13}C{^{1}H} NMR (125 MHz, CD_3CN): δ 142.8, 131.7, 127.8, 97.8, 26.3, 14.4, 9.4. IR (solid): 2332 cm^{-1} (M–N≡*C*-R), 2183 cm^{-1} (M-*C*≡*N*-Ar). *Anal.* Calc. for $C_{23}H_{31}ClF_6IrN_2P$: C, 39.01; H, 4.41; N, 3.95. Found: C, 39.07; H, 4.27; N, 3.87%.

4.18. Synthesis of $[Cp^*IrI(MeCN)(CN\text{-}2,6\text{-}EtC_6H_4)]PF_6$, **1b'[PF$_6$]**

The synthesis is analogous to **1a[PF$_6$]**; Yield 87%. ^{1}H NMR (400 MHz, CD_3CN): δ 7.39 (t, 1H), 7.28 (d, 2H), 2.85 (q, 4H), 2.04 (s, 15H), 1.96 (s, 3H), 1.26 (t, 6H). ^{13}C{^{1}H} NMR (125 MHz, CD_3CN): δ 142.9, 131.6, 127.8, 98.5, 26.3, 14.7, 10.3. IR (solid): 2331 cm^{-1} (M–N≡C-R), 2175 cm^{-1} (M-*C*≡*N*-Ar). *Anal.* Calc. for $C_{23}H_{31}F_6IIrN_2P$: C, 34.54; H, 3.90; N, 3.50. Found: C, 35.20; H, 3.96; N, 3.48%.

4.19. Synthesis of [Cp*RhI(MeCN)(CN-2,6-Xyl)]PF_6, **2b[PF_6]**

The synthesis is analogous **1a[PF_6]**; Yield 85%. ^{1}H NMR (400 MHz, CD_3CN): δ 7.34 (q, 1H), 7.25 (d, 2H), 2.48 (s, 6H), 2.02 (s, 15H), 1.96 (s, 3H). $^{13}C\{^1H\}$ NMR (125 MHz, CD_3CN): δ 137.1, 131.4, 129.2, 104.4, 19.1, 10.9. IR (solid): 2326 cm^{-1} (M–N≡*C*-R), 2182 cm^{-1} (M–*C*≡*N*–Ar). *Anal.* Calc. for $C_{21}H_{27}F_6IN_2PRh$: C, 36.97; H, 3.98; N, 4.10. Found: C, 37.17; H, 3.91; N, 3.71%.

4.20. Synthesis of [Cp*RhCl(MeCN)]$_2$[PF_6]$_2$, **4**

The synthesis is analogous to **1a[PF_6]**; yield 97%. ^{1}H NMR (400 MHz, CD_3CN): δ 1.96 (s, 6H), 1.67 (s, 30H). $^{13}C\{^1H\}$ NMR (125 MHz, CD_3CN): δ 97.94, 8.5. IR (solid): 2232 cm^{-1}, 2294 cm^{-1} (M–N≡*C*-R). *Anal.* Calc.. for $C_{24}H_{36}Cl_2F_{12}N_2P_2Rh_2$: C, 31.36; H, 3.95; N, 3.05. Found: C, 31.59; H, 3.82; N, 2.92%.

4.21. Synthesis of [Cp*Rh(MeCN)$_3$,PF_6]$_2$, **5**

The synthesis is analogous to the reported procedure [49]. crude yield ⩾ 99%. Purified yield 84%. *Anal.* Calc. for $C_{16}H_{24}F_{12}N_3P_2Rh$: C, 29.51; H, 3.71; N, 6.45. Found: C, 29.56; H, 3.53; N, 6.38%.

Acknowledgement

This work was supported by the National Science Foundation, grant CHE-1012405.

Appendix A. Supplementary material

CCDC 939777–939796 contain the supplementary crystallographic data for this paper. These data can be obtained free of charge from The Cambridge Crystallographic Data Centre via http://www.ccdc.cam.ac.uk/data_request/cif. Supplementary data associated with this article can be found, in the online version, at http://dx.doi.org/10.1016/j.ica.2013.07.039.

References

[1] C–H activation, in: J.-Q. Yu, Z. Shi (Eds.), Topics in Current Chemistry, vol. 292, Springer, Berlin, Germany, 2010.
[2] G. Dyker, Handbook of C–H Transformations, Wiley-VCH, Weinheim, 2005.
[3] Activation of unreactive bonds and organic synthesis, in: S. Murai (Ed.), Topics in Organometallic Chemistry, vol. 3, Springer, Berlin, Germany, 1999.
[4] J. Alvarez-Builla, J.J. Vaquero, J. Barluenga (Eds.), Modern Heterocyclic Chemistry, Wiley-VCH, Weinheim, Germany, 2011.
[5] O. Baudoin, Chem. Soc. Rev. 40 (2011) 4902.
[6] R. Jazzar, J. Hitce, A. Renaudat, J. Sofack-Kreutzer, O. Baudion, Chem. Eur. J. 16 (2010) 2654.
[7] M. Albrecht, Chem Rev. 110 (2010) 576.
[8] D.A. Colby, R.G. Bergman, J.A. Ellman, Chem. Rev. 110 (2010) 624.
[9] G.E. Dobereiner, R.H. Crabtree, Chem. Rev. 110 (2010) 681.
[10] M.C. Willis, Chem Rev. 110 (2010) 725.
[11] P. Sehnal, R.J.K. Taylor, I.J.S. Fairlamb, Chem. Rev. 110 (2010) 824.
[12] I.A.I. Mkhalid, J.H. Barnard, T.B. Marder, J.M. Murphy, J.F. Hartwig, Chem. Rev. 110 (2010) 890.
[13] A. Gunay, K.H. Theopold, Chem. Rev. 110 (2010) 1060.
[14] T.W. Lyons, M.S. Sanford, Chem. Rev. 110 (2010) 1147.
[15] J. Granell, M. Martinez, Dalton Trans. 41 (2012) 11243.
[16] D. Lapointe, K. Fagnou, Chem. Lett. 39 (2010) 1118.
[17] D. Balcells, E. Clot, O. Eisenstein, Chem. Rev. 110 (2010) 749.
[18] Y. Boutadla, D.L. Davies, S.A. Macgregor, A.I. Poblador-Baha-Monde, Dalton Trans (2009) 5820.
[19] L. Ackermann, Chem. Rev. 111 (2011) 1315.
[20] K. Fagnou, Top Curr. Chem. 292 (2010) 35.
[21] S. Gorelsky, D. Lapointe, K. Fagnou, J. Am. Chem. Soc. 130 (2008) 10848.
[22] L. Ackermann, Acc. Chem. Res. (2013), http://dx.doi.org/10.1021/ar3002798.
[23] R. Vicente, L. Ackermann, Top Curr. Chem. 292 (2010) 211.
[24] L. Ackermann, R. Vicente, H.K. Potukuchi, V. Pirovano, Org. Lett. 12 (2010) 5032.
[25] L. Ackermann, R. Vicente, A. Althammer, Org. Lett. 10 (2008) 2299.
[26] J.A. Ellman, R.G. Bergman, Y. Lian, T. Huber, K.D. Hesp, Angew. Chem., Int. Ed. 52 (2013) 629.
[27] J.A. Ellman, R.G. Bergman, M.E. Tauchert, C.D. Incarvito, A.L. Rheingold, J. Am. Chem. Soc. 134 (2012) 1482.
[28] J.A. Ellman, R.G. Bergman, D.A. Colby, A.S. Tsai, Acc. Chem. Res. 45 (2012) 814.
[29] J.A. Ellman, R.G. Bergman, Y. Lian, Chem. Sci. 3 (2012) 3088.
[30] J.A. Ellman, R.G. Bergman, K.D. Hesp, Org. Lett. 14 (2012) 2304.
[31] J.A. Ellman, R.G. Bergman, M. Brasse, A.S. Tsai, Org. Lett. 13 (2011) 540.
[32] L. Li, W.W. Brennessel, W.D. Jones, J. Am. Chem. Soc. 130 (2008) 12414.
[33] L. Li, W.W. Brennessel, W.D. Jones, Organometallics 28 (2009) 3492.
[34] L. Li, Y. Jiao, W.W. Brennessel, W.D. Jones, Organometallics 29 (2010) 4593.
[35] J.M. Rhinehart, K.A. Manbeck, S.K. Buzak, G.M. Lippa, W.W. Brennessel, K.I. Goldberg, W.D. Jones, Organometallics 31 (2012) 1943.
[36] M. Paneque, K. Mereiter, L.L. Santos, Organometallics 32 (2013) 565.
[37] E. Carmona, L.L. Santos, M.L. Poveda, M. Paneque, S. Canejero, Acc. Chem. Res. 43 (2010) 572.
[38] P. Lara, M. Paneque, M.L. Poveda, L.L. Santos, J.E.V. Valpuesta, E. Carmona, S. Moncho, G. Ujaque, A. Lledós, E. Álvarez, K. Mereiter, Chem. Eur. J. 15 (2009) 9034.
[39] E. Carmona, J. Campos, A.C. Esqueda, Chem Eur. J. 16 (2010) 419.
[40] W.P. Kosar, W.D. Jones, J. Am. Chem. Soc. 108 (1986) 5640.
[41] G.C. Hsu, W.P. Kosar, W.D. Jones, Organometallics 13 (1994) 385.
[42] J.W. Kang, K. Moseley, P.M. Matilis, J. Am. Chem. Soc. 91 (1969) 5970.
[43] F. Farone, V. Marsala, G. Tresoldi, J. Organomet. Chem. 152 (1978) 337.
[44] W.D. Jones, R.P. Duttweiler Jr., F.J. Feher, Inorg. Chem. 29 (1990) 1505.
[45] D. Carmona, J. Ferrer, L.A. Oro, Organometallics 12 (1993) 4241.
[46] E.G. Fidalgo, A. Neels, H. Stoeckli-Evans, G. Süss-Fink, J. Organomet. Chem. 602 (2000) 188.
[47] C.G. Hartinger, Organometallics 28 (2009) 6260.
[48] A. Neels, H. Stoeckli-Evans, L. Plasseraud, E.G. Fidalgo, G. Süss-Fink, Acta Cryst. C55 (1999) 2030. The previously reported crystal structure has been crystallized with a mole of toluene. The structure reported here (**3′**), in the SI, is unique and crystallized without solvent.
[49] C. White, S.J. Thompson, P.M. Maitlis, Dalton Trans. (1977) 1654. While the compound has been synthesized and reported there has been no reported crystal structure and has been submitted with this report in the SI; a = 14.998(2) Å, b = 33.347(5) Å, c = 33.711(6) Å; α = 119.481(3)°, β = 90.660(3)°, γ = 90.366(3)°.
[50] T. Mathieson, A. Schier, H. Schmidbaur, J. Chem. Soc., Dalton Trans. (2001) 1196.
[51] R.K. Castellano, F. Diederich, E.A. Meyer, Angew. Chem., Int. Ed. 42 (2003) 1210.
[52] W.P. Kosar, W.D. Jones, Organometallics 5 (1986) 1823.
[53] B. Kim, J.M. Beebe, Y. Jun, X.-Y. Zhu, C.D. Frisbie, J. Am. Chem. Soc. 129 (2006) 4970.